

# Exploration of rare earth doped zirconia aerogels for high temperature aerospace applications

**Nathaniel Olson**<sup>1</sup>, Dr. Frances Hurwitz<sup>2\*</sup>, Dr. Jamesa Stokes<sup>2</sup>,  
Dr. Haiquan Guo<sup>3</sup>, Dr. Jessica Krogstad<sup>1</sup>

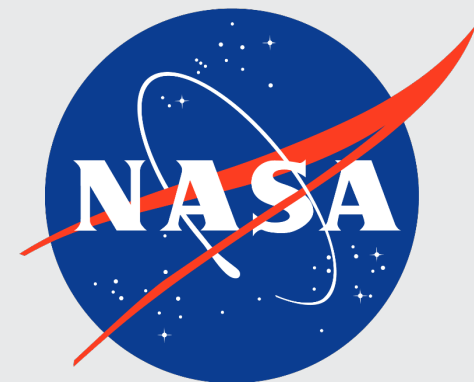
<sup>1</sup>University of Illinois at Urbana-Champaign, Department of Materials Science and Engineering, Urbana, IL

<sup>2</sup>NASA Glenn Research Center, Cleveland, OH

<sup>3</sup>Universities Space Research Association, Cleveland, OH

\* Retired

46<sup>th</sup> International Conference on Advanced Ceramics and Composites  
Porous Ceramics: Novel Developments and Applications  
Engineering Applications of Porous Ceramics II  
January 25<sup>th</sup>, 2022



This work is supported by a NASA Space Technology Research Fellowship

# Developing lightweight, high performance insulation for aerospace applications



NASA's estimated cost to launch into low Earth orbit is approximately **\$5000 per kilogram**

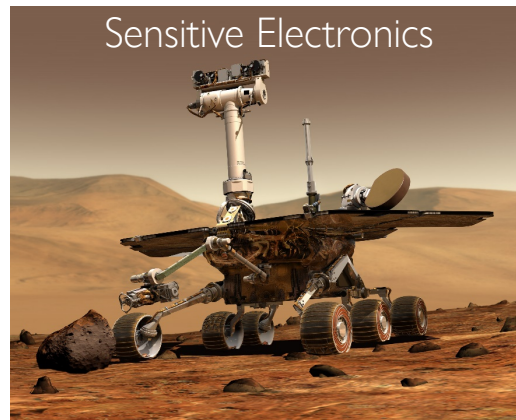
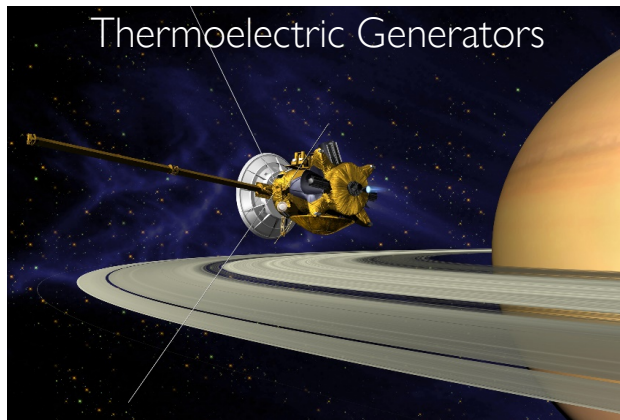


10% reduction in mass of thermal protection system =

**\$4,300,000 reduction in cost per launch**

For the Space Shuttle program

- 1) Lower thermal conductivity → improve insulative performance
- 2) Reduce mass and/or volume → reduce cost, improve payload capacity

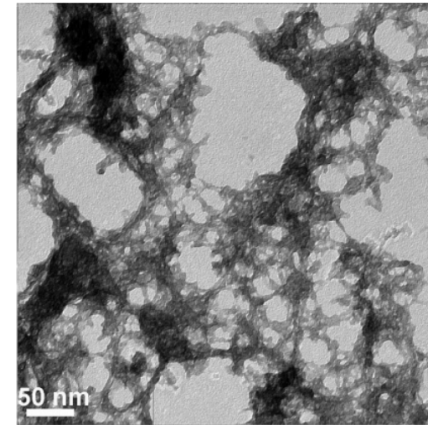


# Aerogels are highly insulating and lightweight materials

- High specific surface area (SSA), high porosity, and low density
  - **SSA:** 200 – 1000 m<sup>2</sup>/g
  - **Porosity:** 90 – 99.9%
- Low thermal conductivity
  - Low as 0.009 W/(m•K) in atmosphere and 0.003 W/(m•K) under vacuum
  - Low density = **Low solid conductivity**
  - Pore sizes ≤ mean free path of gas = **Low gas convection**
- Versatile synthesis adaptable to a wide array of metal oxide compositions
- Incorporate ceramic fibers/felts/papers with aerogel to reinforce for insulation

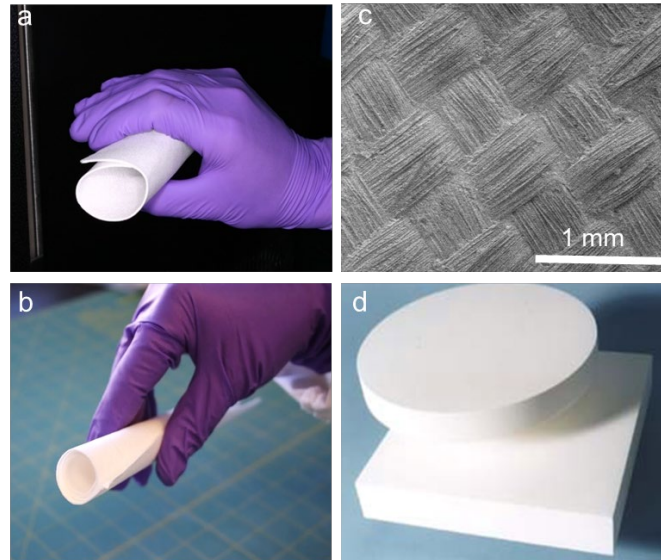


Bunsen burner applied to aerogel (LANL)



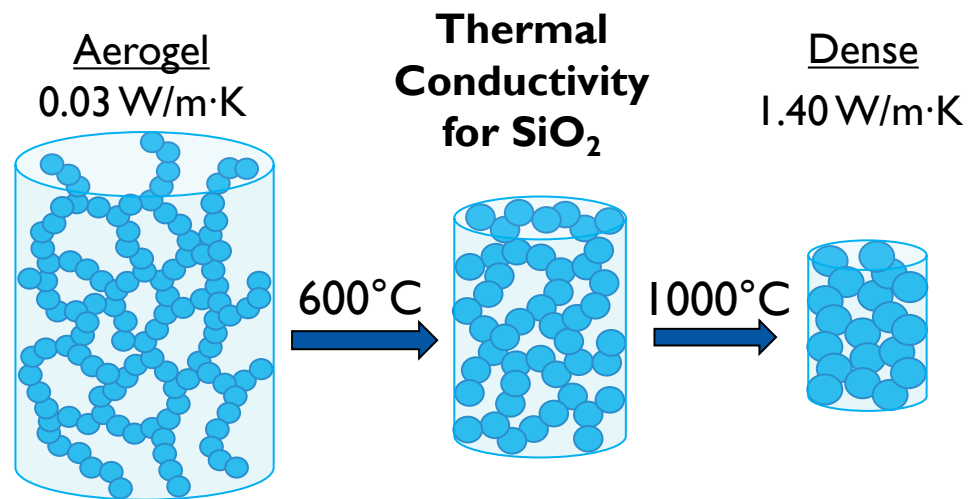
Highly porous network of interconnected nanoparticles

Highly porous structure of aerogel is responsible for its extremely low thermal conductivity.



Various aerogel composite materials using alumina or aluminosilicate reinforcements

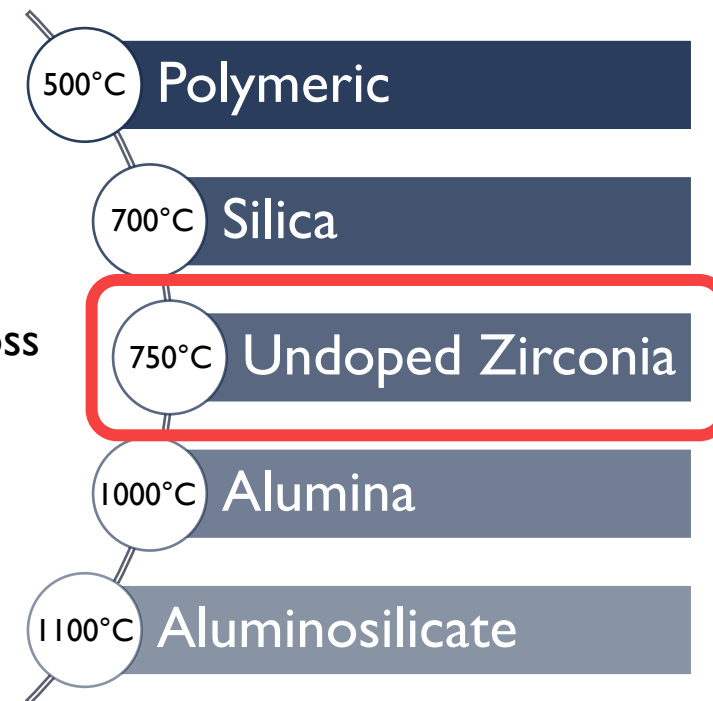
# Collapse of pore structure and loss of favorable properties occurs upon exposure to high temperatures



Loss of SSA, porosity  
↑ thermal conductivity,  
cracking, and shrinkage

Large SSA & porosity contribute  
to driving force for densification

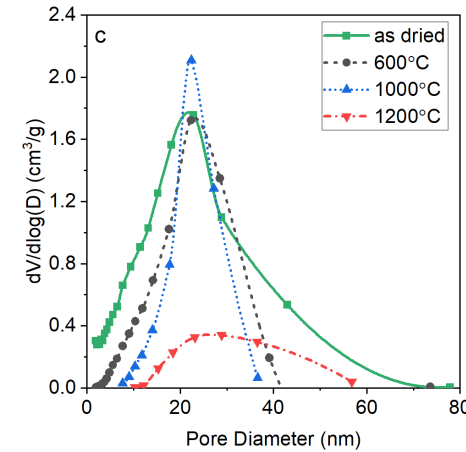
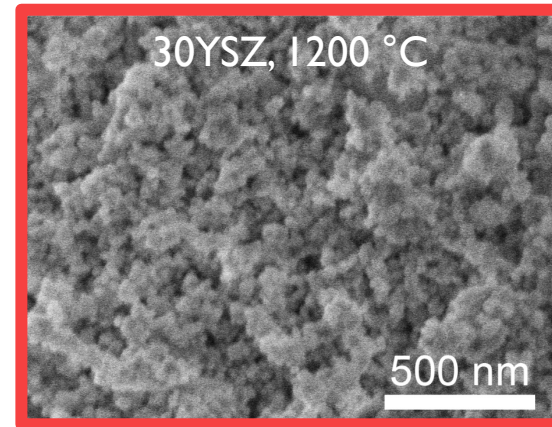
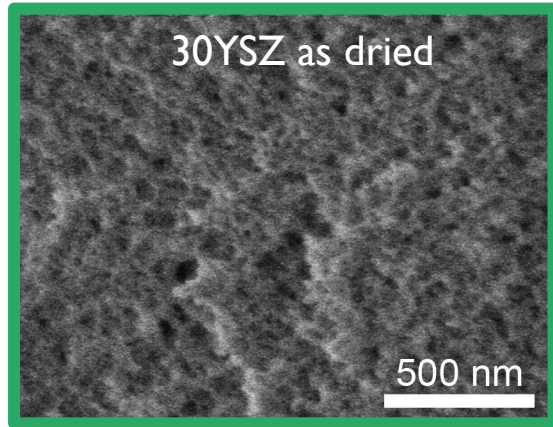
Rapid densification & loss  
of porosity beyond...



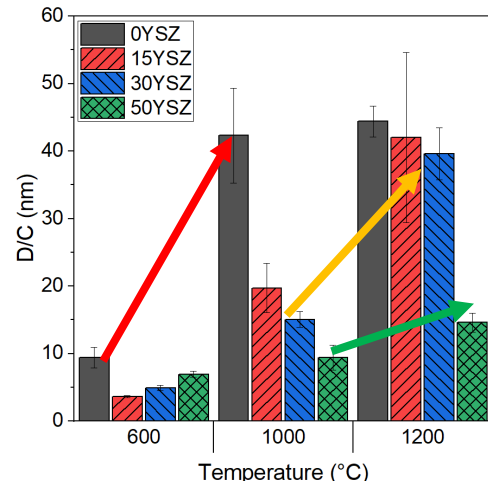


# High yttria concentration improves thermal stability

## 1. Reduces densification of the pore structure (SEM, N<sub>2</sub> physisorption)



## 2. Suppresses crystallite growth to 1200 °C (XRD, TEM)



By what mechanism is yttria improving the thermal stability of the pore structure?

**Thermodynamics**  
(Lower Surface Energy)

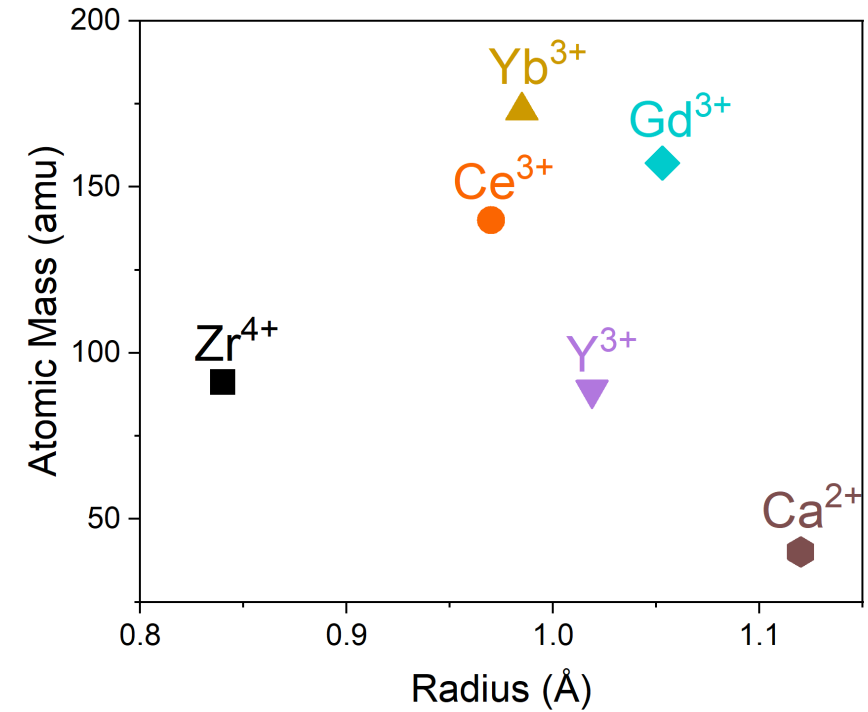
**Kinetics**  
(Lower Cation Diffusivity)

# Study of other dopants (Y, Yb, Gd, Ca, Ce) in zirconia aerogels at 15 and 30 mol% M/(M+Zr)

Further exploration of dopant properties (size, mass, charge) on aerogel thermal stability

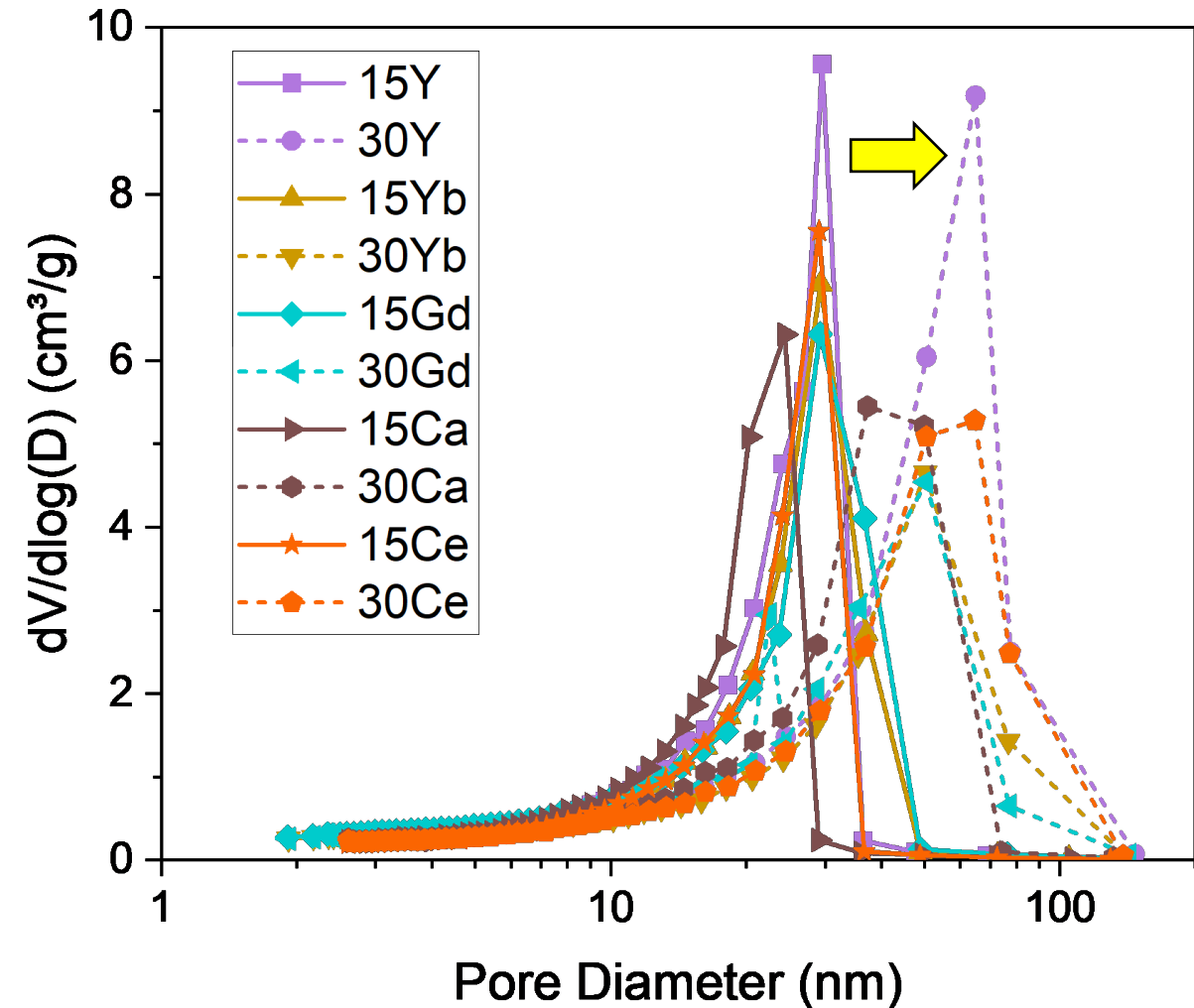
Periodic Table of the Elements

1 IA 1A 1 H Hydrogen 1.008	2 IIA 2A 4 Be Beryllium 9.012																	18 VIIIA 8A 2 He Helium 4.003																	
3 Li Lithium 6.941	11 Na Sodium 22.990	12 Mg Magnesium 24.305	13 Al Aluminum 26.982	14 Si Silicon 28.086	15 P Phosphorus 30.974	16 S Sulfur 32.066	17 Cl Chlorine 35.453	18 Ar Argon 39.948	19 K Potassium 39.098	20 Ca Calcium 40.078	21 Sc Scandium 44.956	22 Ti Titanium 47.867	23 V Vanadium 50.942	24 Cr Chromium 51.996	25 Mn Manganese 54.938	26 Fe Iron 55.845	27 Co Cobalt 58.933	28 Ni Nickel 58.693	29 Cu Copper 63.546	30 Zn Zinc 65.38	31 Ga Gallium 69.723	32 Ge Germanium 72.631	33 As Arsenic 74.922	34 Se Selenium 78.971	35 Br Bromine 79.904	36 Kr Krypton 83.798									
37 Rb Rubidium 85.468	38 Sr Strontium 87.62	39 Y Yttrium 88.906	40 Zr Zirconium 91.224	41 Nb Niobium 92.906	42 Mo Molybdenum 95.95	43 Tc Technetium 98.907	44 Ru Ruthenium 101.07	45 Rh Rhodium 102.906	46 Pd Palladium 106.42	47 Ag Silver 107.868	48 Cd Cadmium 112.414	49 In Indium 114.818	50 Sn Tin 118.711	51 Sb Antimony 121.760	52 Te Tellurium 127.6	53 I Iodine 126.904	54 Xe Xenon 131.294	55 Cs Cesium 132.905	56 Ba Barium 137.328	57-71 Lanthanide Series	72 Hf Hafnium 178.49	73 Ta Tantalum 180.948	74 W Tungsten 183.84	75 Re Rhenium 186.207	76 Os Osmium 190.23	77 Ir Iridium 192.217	78 Pt Platinum 195.085	79 Au Gold 196.967	80 Hg Mercury 200.592	81 Tl Thallium 204.383	82 Pb Lead 207.2	83 Bi Bismuth 208.980	84 Po Polonium [208.982]	85 At Astatine [209.987]	86 Rn Radon 222.018
87 Fr Francium 223.020	88 Ra Radium 226.025	89-103 Actinide Series	104 Rf Rutherfordium [261]	105 Db Dubnium [262]	106 Sg Seaborgium [266]	107 Bh Bohrium [264]	108 Hs Hassium [269]	109 Mt Meitnerium [278]	110 Ds Darmstadtium [281]	111 Rg Roentgenium [280]	112 Cn Copernicium [285]	113 Nh Nihonium [286]	114 Fl Flerovium [289]	115 Mc Moscovium [289]	116 Lv Livermorium [293]	117 Ts Tennessine [294]	118 Og Oganesson [294]																		
57 La Lanthanum 138.905	58 Ce Cerium 140.116	59 Pr Praseodymium 140.908	60 Nd Neodymium 144.243	61 Pm Promethium 144.913	62 Sm Samarium 150.36	63 Eu Europium 151.964	64 Gd Gadolinium 157.25	65 Tb Terbium 158.925	66 Dy Dysprosium 162.500	67 Ho Holmium 164.930	68 Er Erbium 167.259	69 Tm Thulium 168.934	70 Yb Ytterbium 173.055	71 Lu Lutetium 174.967																					
89 Ac Actinium 227.028	90 Th Thorium 232.038	91 Pa Protactinium 231.036	92 U Uranium 238.029	93 Np Neptunium 237.048	94 Pu Plutonium 244.064	95 Am Americium 243.061	96 Cm Curium 247.070	97 Bk Berkelium 247.070	98 Cf Californium 251.080	99 Es Einsteinium [254]	100 Fm Fermium 257.095	101 Md Mendelevium 258.1	102 No Nobelium 259.101	103 Lr Lawrencium [262]																					

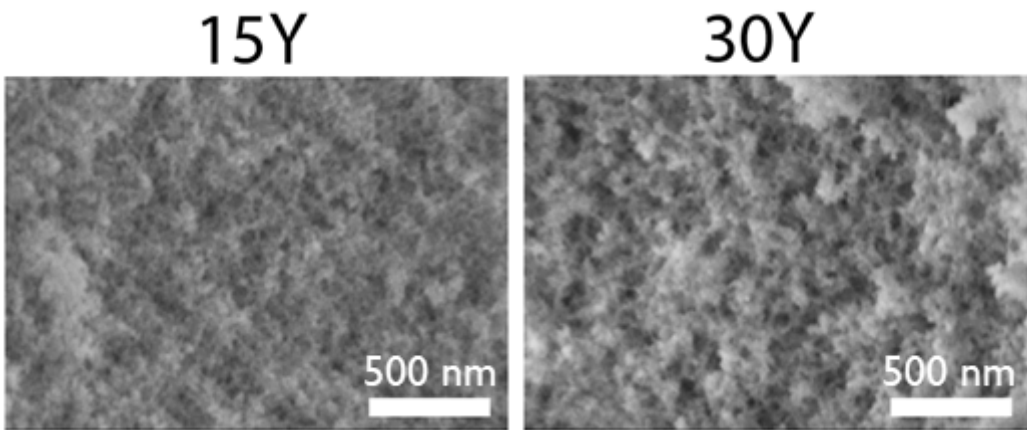


→ Modify thermal conductivity, surface energy and cation diffusivity  
 → Connect material properties to changes in structural evolution

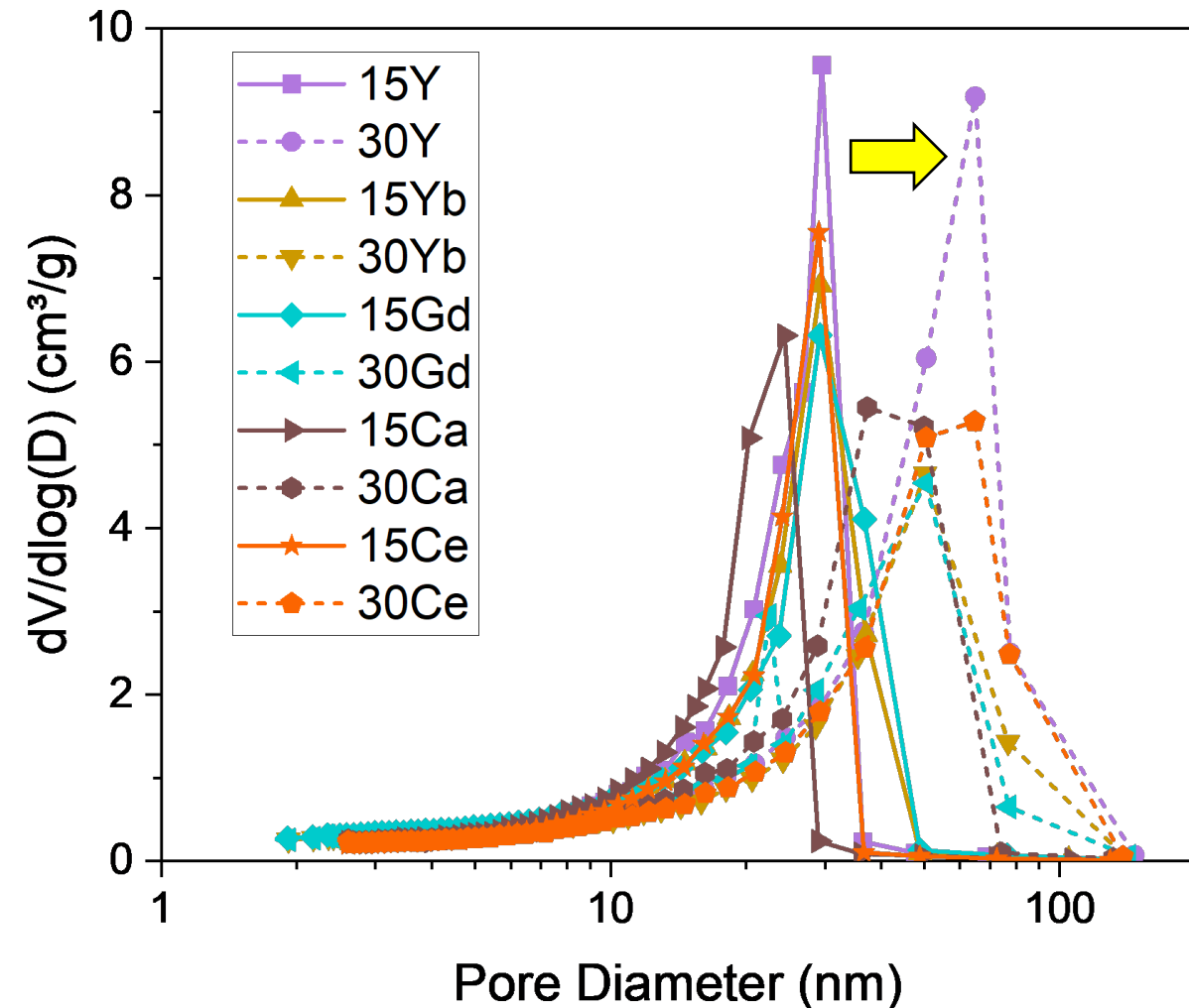
# As dried structure characterized with nitrogen physisorption and SEM



Increased dopant concentration from 15 to 30 mol% increases average pore size and distribution breadth for *all* dopants.



# Change in average metal oxidation state hypothesized to increase distribution breadth at 30 mol% dopant



From 15 to 30 mol% dopant we replace more  $Zr^{4+}$  with cations of lower charge

Average metal oxidation state is decreased

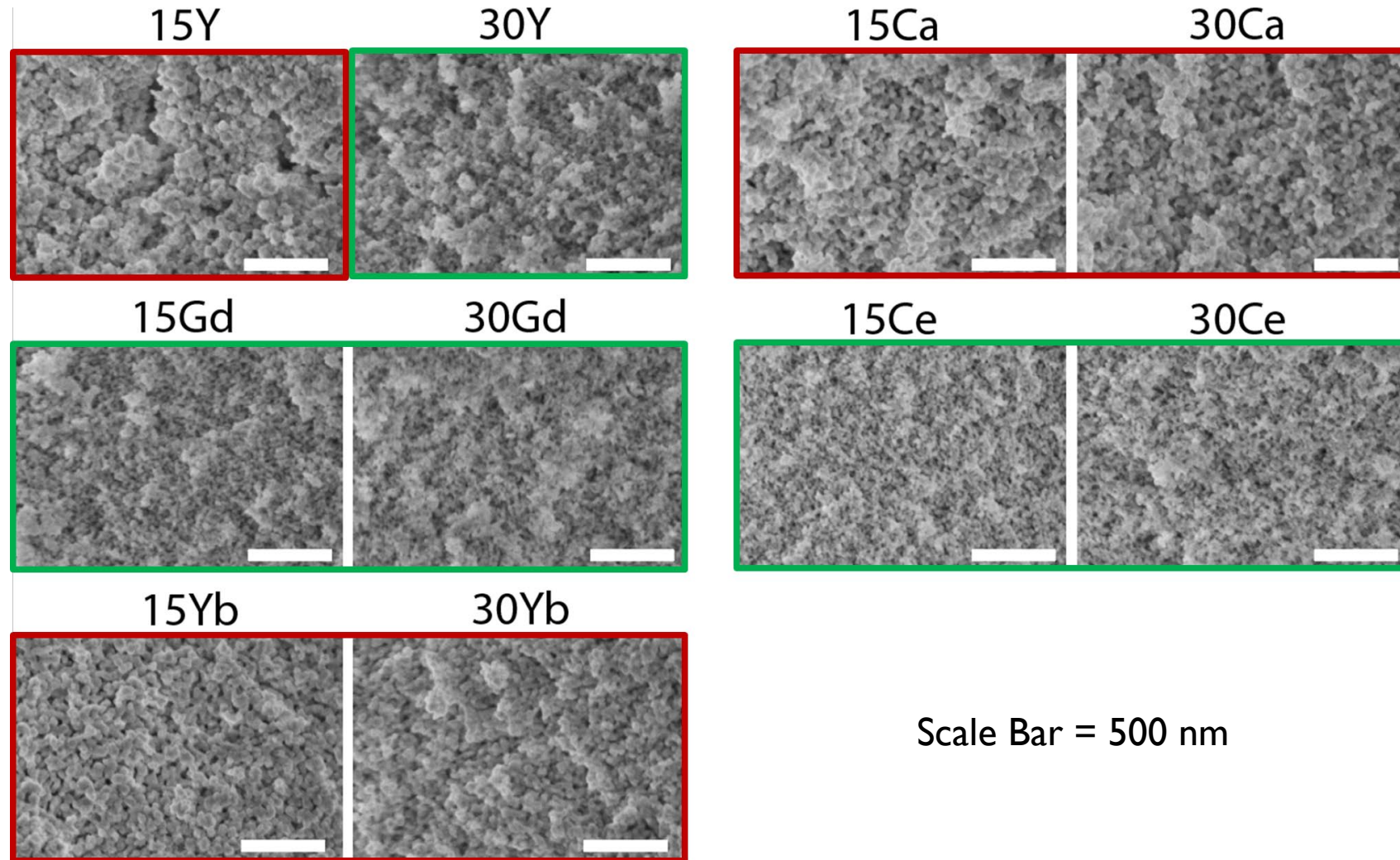
Average acidity of  $[M(H_2O)_x]^{x+}$  is reduced

Reducing the acidity in turn slows down gel formation. This gives more time for nucleation and growth of particles in the sol.

Larger particles cannot pack as closely together, leading to broader pore size distributions with larger average pore size.



# Pore structure stability to 1000 °C appears to be dependent on dopant identity & amount



**Red:** increased particle size and reduction of mesoporosity.  
**Green:** mesoporous structure maintained.

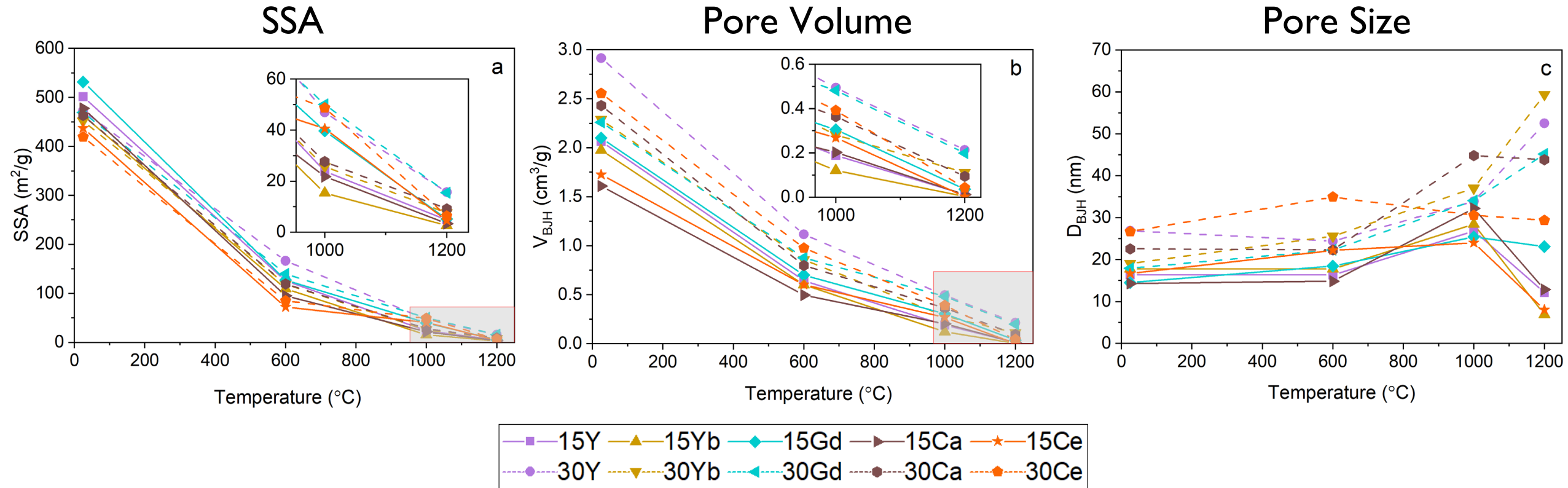
Larger set of samples & temperatures requires quantifiable criteria for “thermally stable” aerogels



Bulk of the work on this study lies in developing these **metrics of thermal stability**

Scale Bar = 500 nm

# Evaluation of pore structure with nitrogen physisorption quantifies change in performance



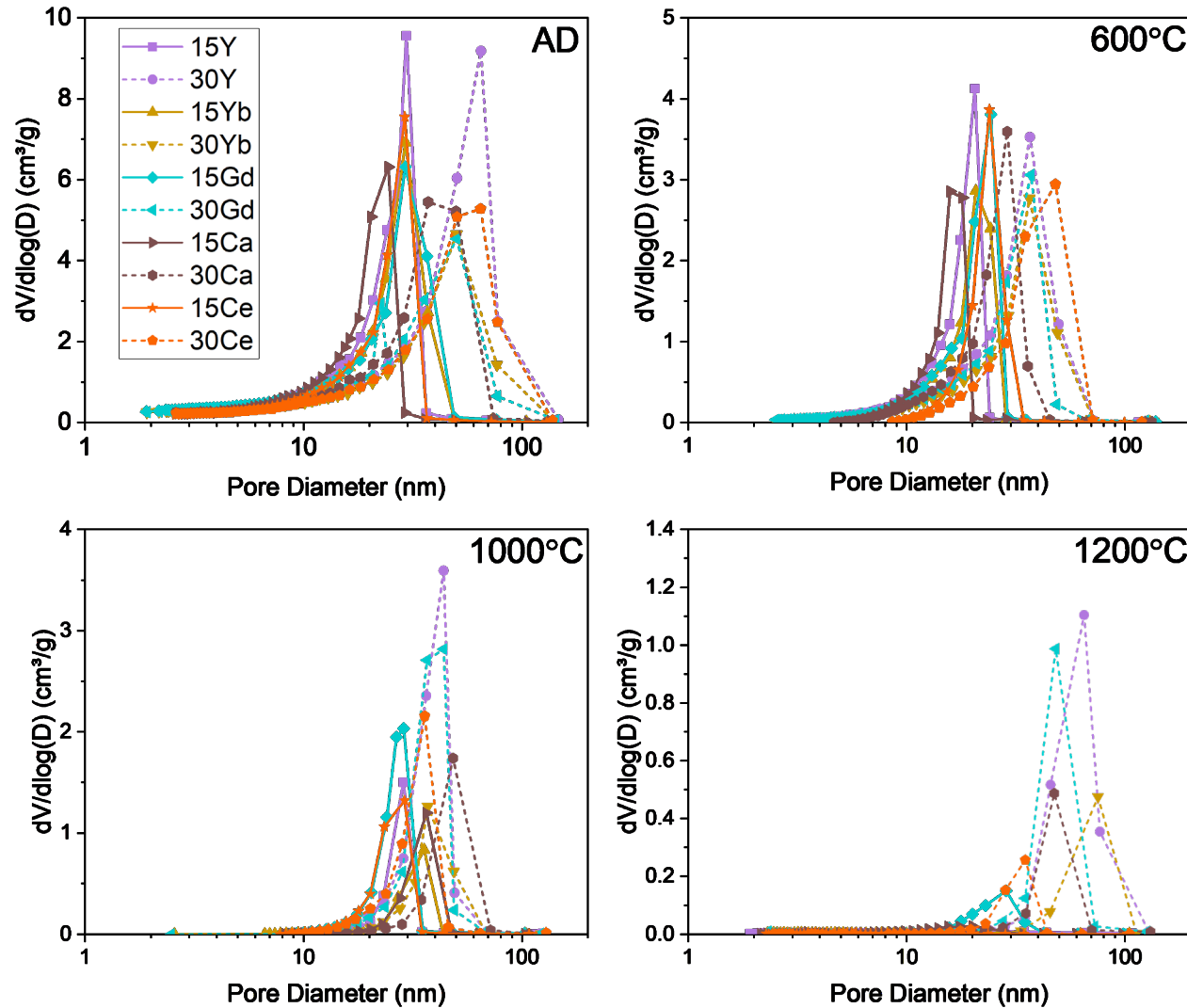
## Best Performers\*

1000 °C: 30Y, 30Gd, 30Ce

1200 °C: 30Y, 30Gd

With 10 samples at 4 different conditions, becomes difficult to discern differences in behavior!

# Increased dopant content improves stability of pore structure to 1200 °C



At 600 °C, no visible difference between 15 and 30 mol% MO<sub>x</sub>

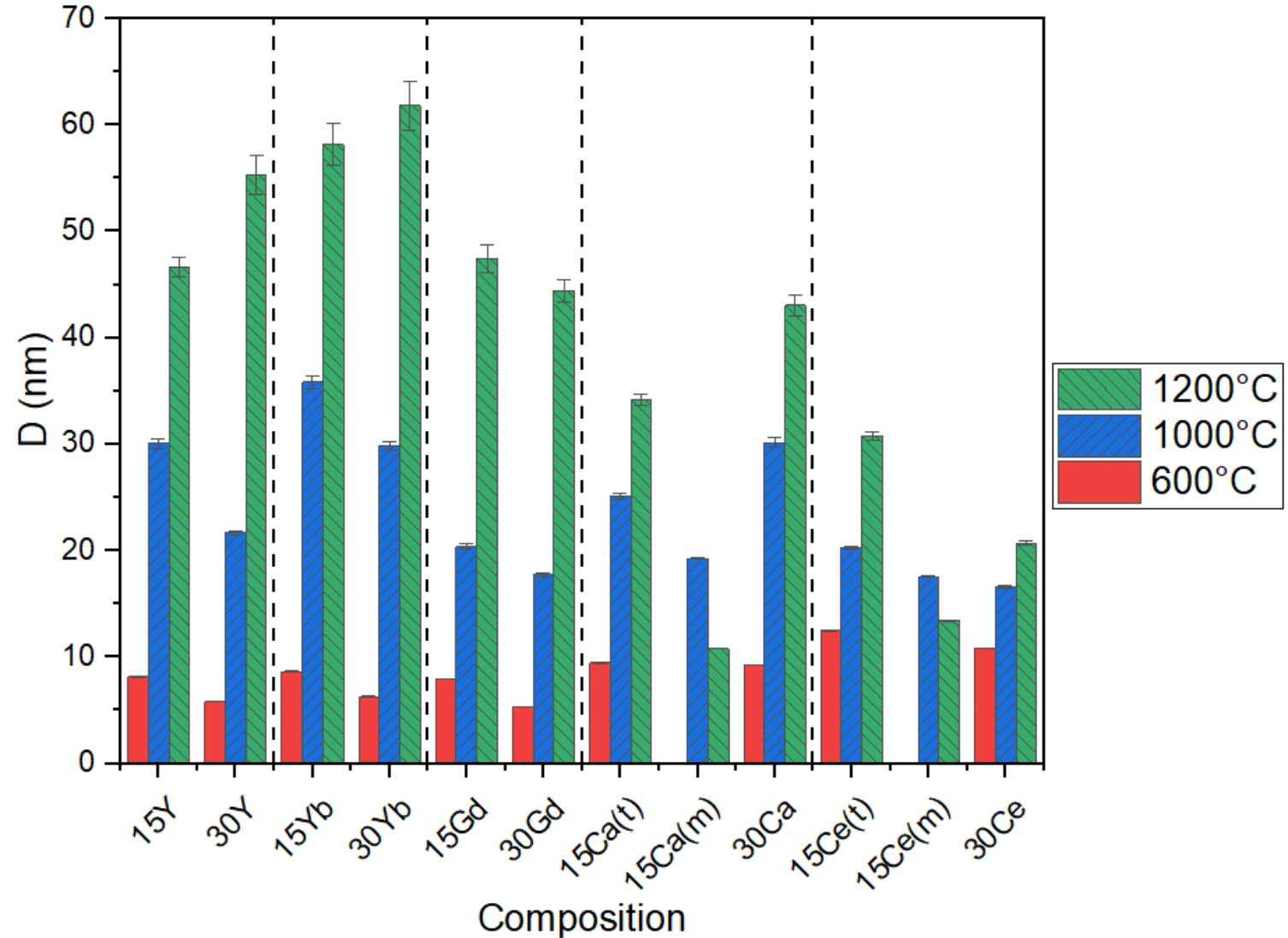
At 1000 and 1200 °C, it becomes apparent 30 mol% MO<sub>x</sub> maintains more porosity. Gd and Y perform the best.

# Crystallite growth quantified as a function of dopant identity and concentration

Trivalent dopants (Y, Yb, Gd) all maintain a single cubic phase at 15 and 30 mol%

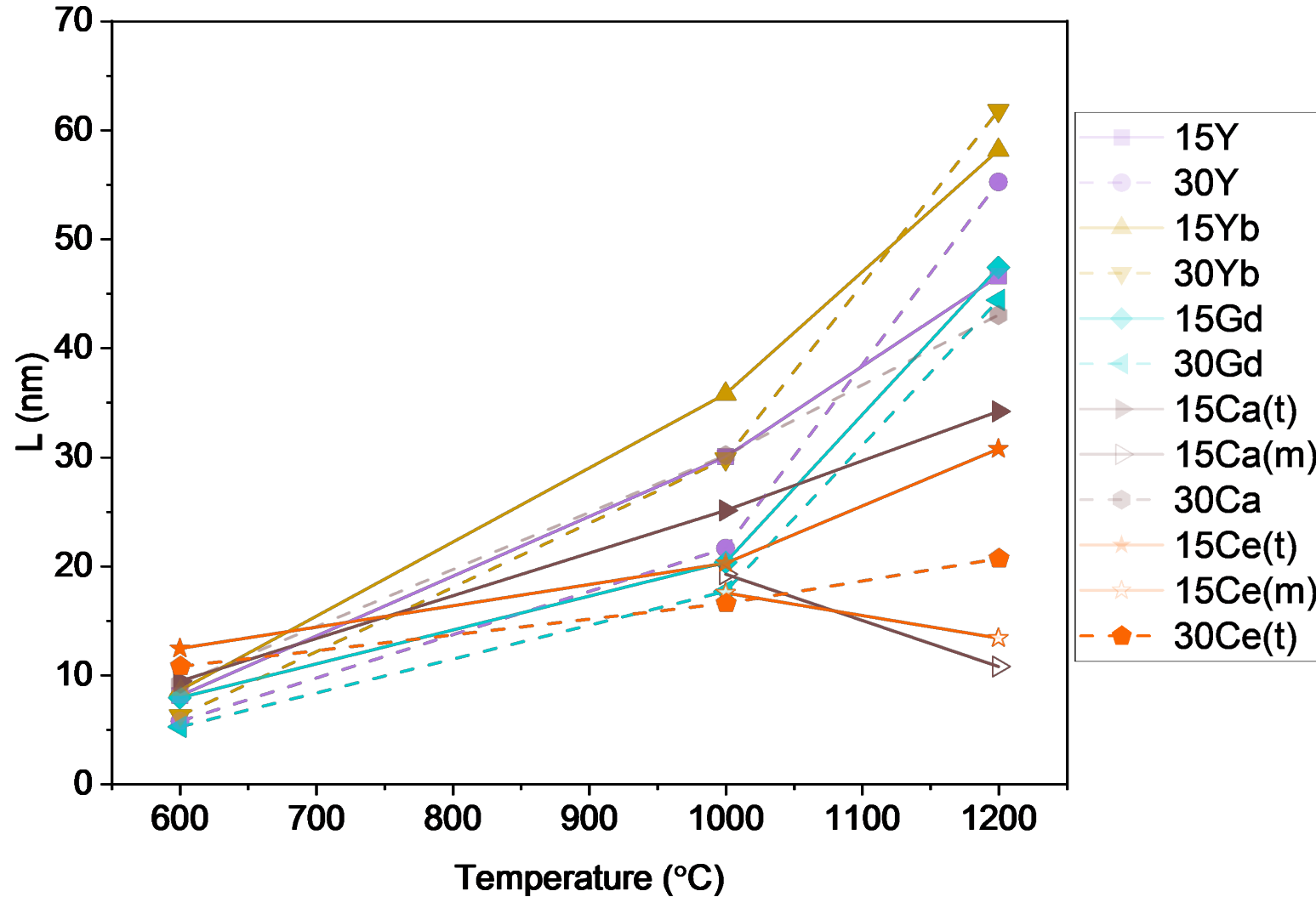
15Ca and 15Ce contain mixed tetragonal and monoclinic phases

30Ca is cubic and 30Ce is tetragonal





# Crystallite growth quantified as a function of dopant identity and concentration



Notable similarity in all trivalent dopants (Y, Yb, Gd) at both 15 and 30 mol%  
**Gd < Y < Yb**

Samples that form mixed tetragonal and monoclinic phases (15Ca, 15Ce) maintain small crystallite size, but have **low phase stability**, which can lead to structure collapse

30Ce maintains a single phase and the smallest crystallite size (by far!) to 1200 °C

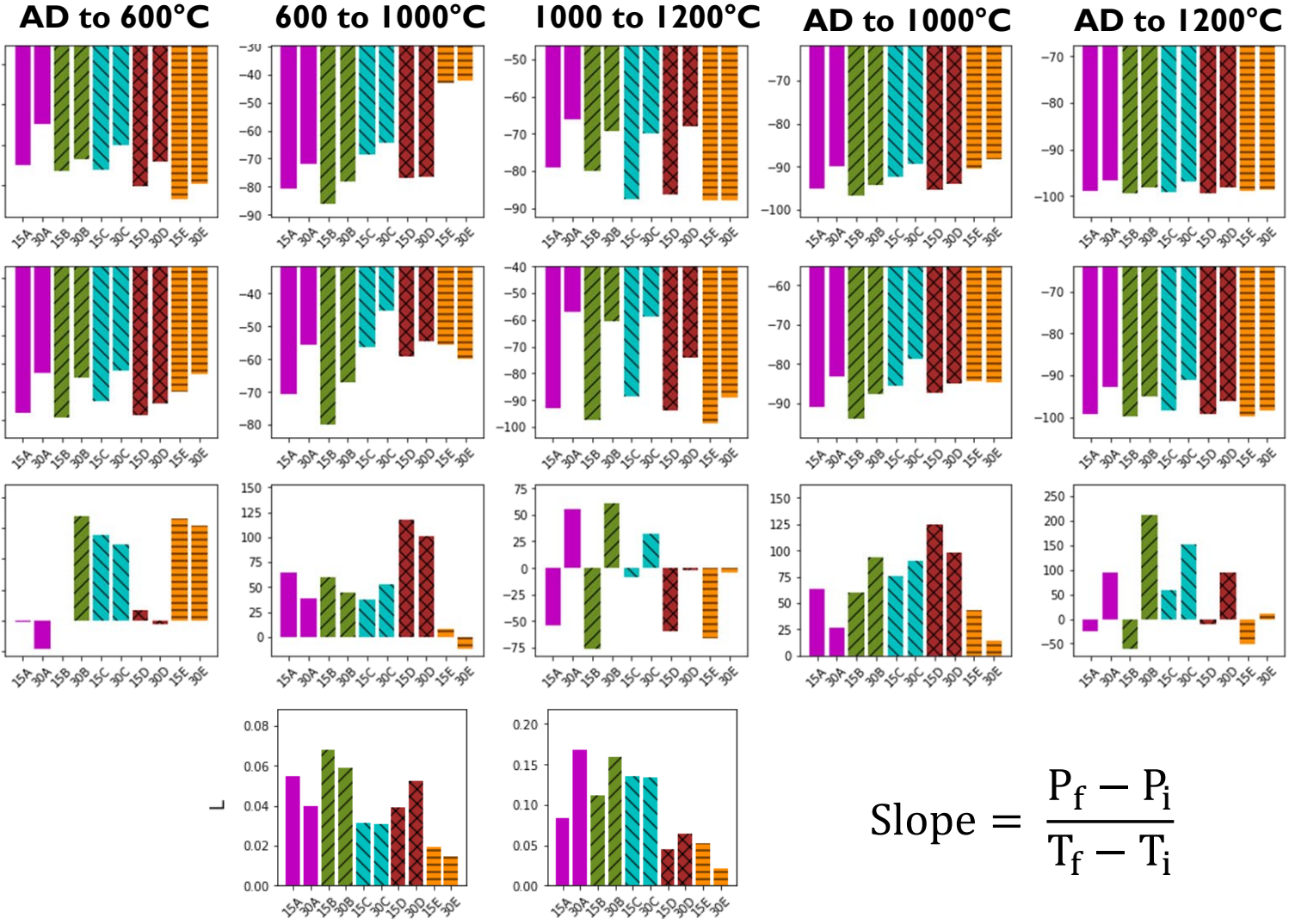
# Evaluation of relative stability via percent change and slope of properties as function of temperature

**Specific Surface Area**

**Pore Volume**

**Pore Size**

**Crystallite Size**



$$\% \text{ Change} = \frac{P_f - P_i}{P_i} \times 100\%$$

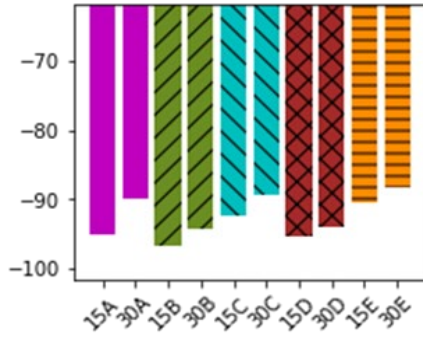
$$\text{Slope} = \frac{P_f - P_i}{T_f - T_i}$$

- A = Y
- B = Yb
- C = Gd
- D = Ca
- E = Ce

# Evaluation of relative stability via percent change and slope of properties as function of temperature

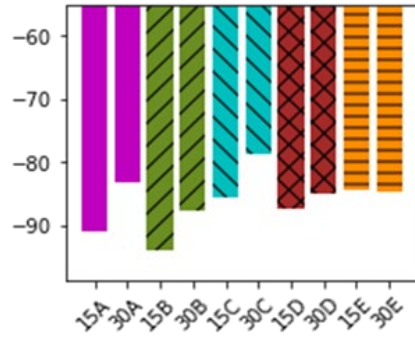
AD to 1000°C

Specific Surface Area



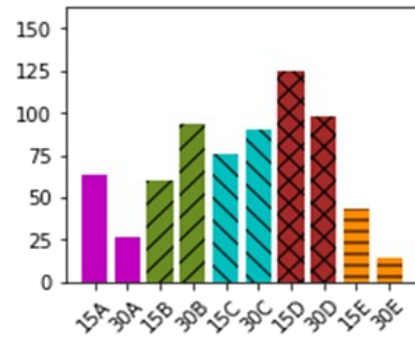
A = Y  
 B = Yb  
 C = Gd  
 D = Ca  
 E = Ce

Pore Volume

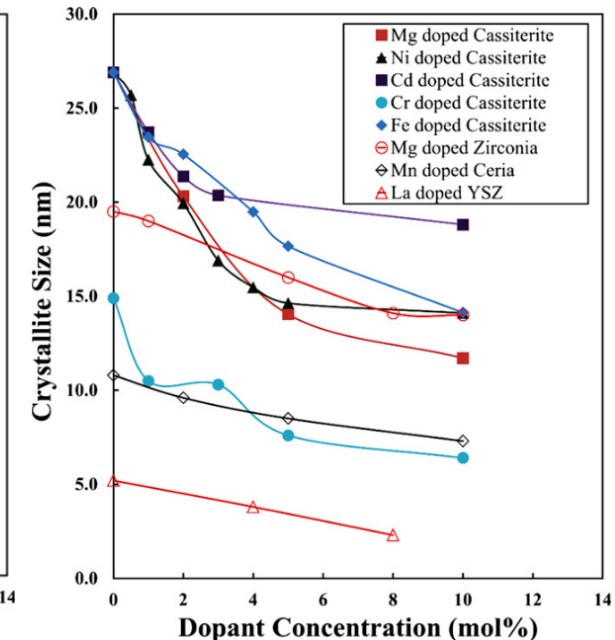
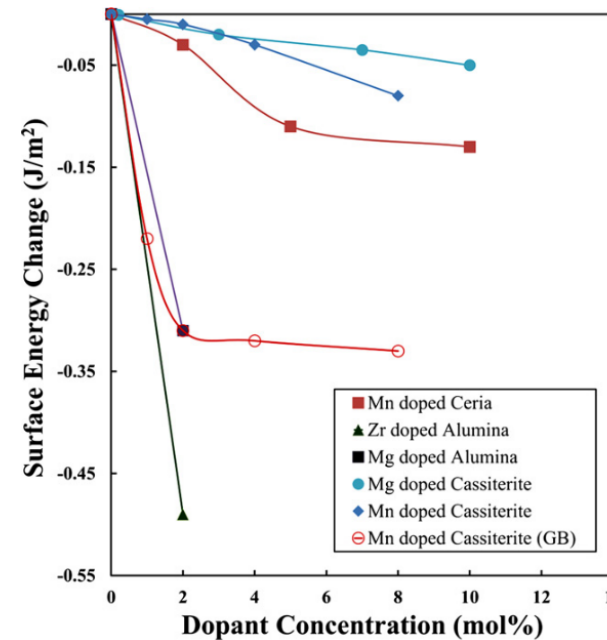


Increased dopant concentration leads to reduced densification.

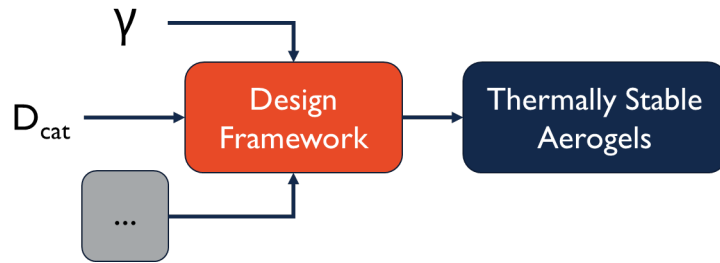
Pore Size



Work in the field of nanocrystalline ceramics suggests dopants can segregate to surfaces, pinning grain boundaries and reducing surface energies and thereby reducing rates of sintering and densification.



# Connecting material properties to thermal stability



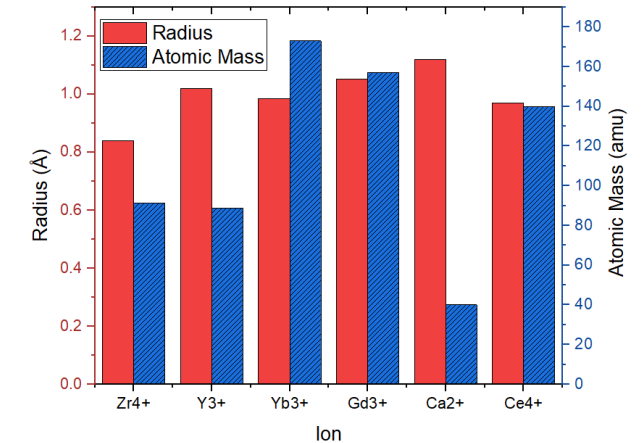
From our work on YSZ, we were able to connect our results to others' measurements of surface energy and cation diffusivity.

But... neither those properties nor others are available for wider ranges of dopants and concentrations

Given this absence, we turned to something readily available: cation properties (mass, radius, charge)

Next, we calculated a weighted average for each material

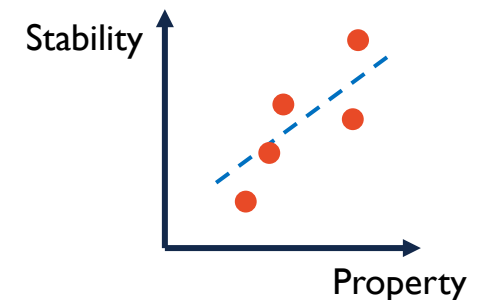
We then performed linear regression on the absolute (SSA, V, D, L at a given temperature) and relative (percent change) thermal stability.



$$\text{Weighted Property} = x_{\text{Zr}} P_{\text{Zr}} + x_{\text{M}} P_{\text{M}}$$

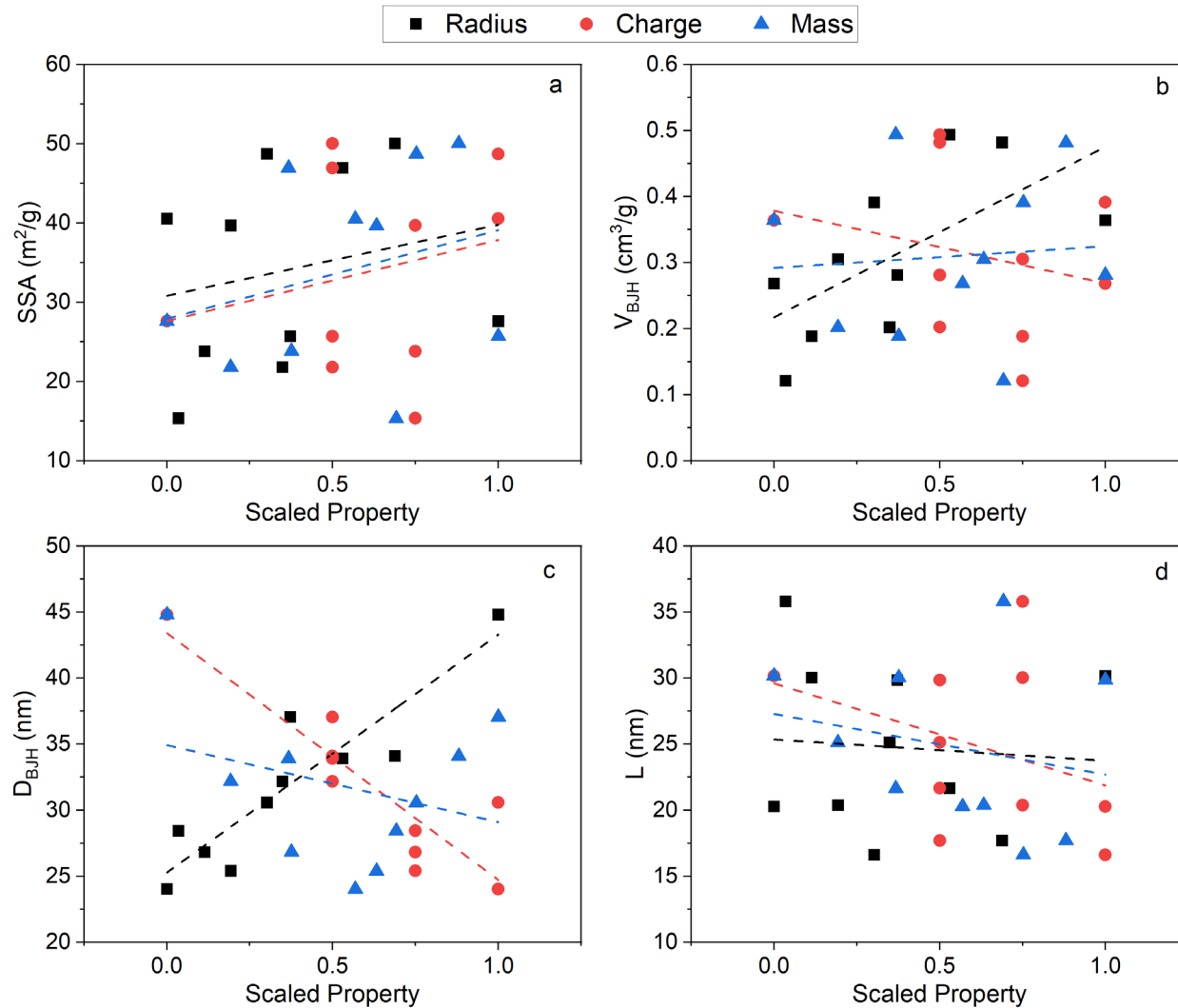
$$x_{\text{M}} = \text{mole fraction } \text{MO}_y$$

$$P_{\text{M}} = \text{property of dopant } \text{M}^{2y+}$$



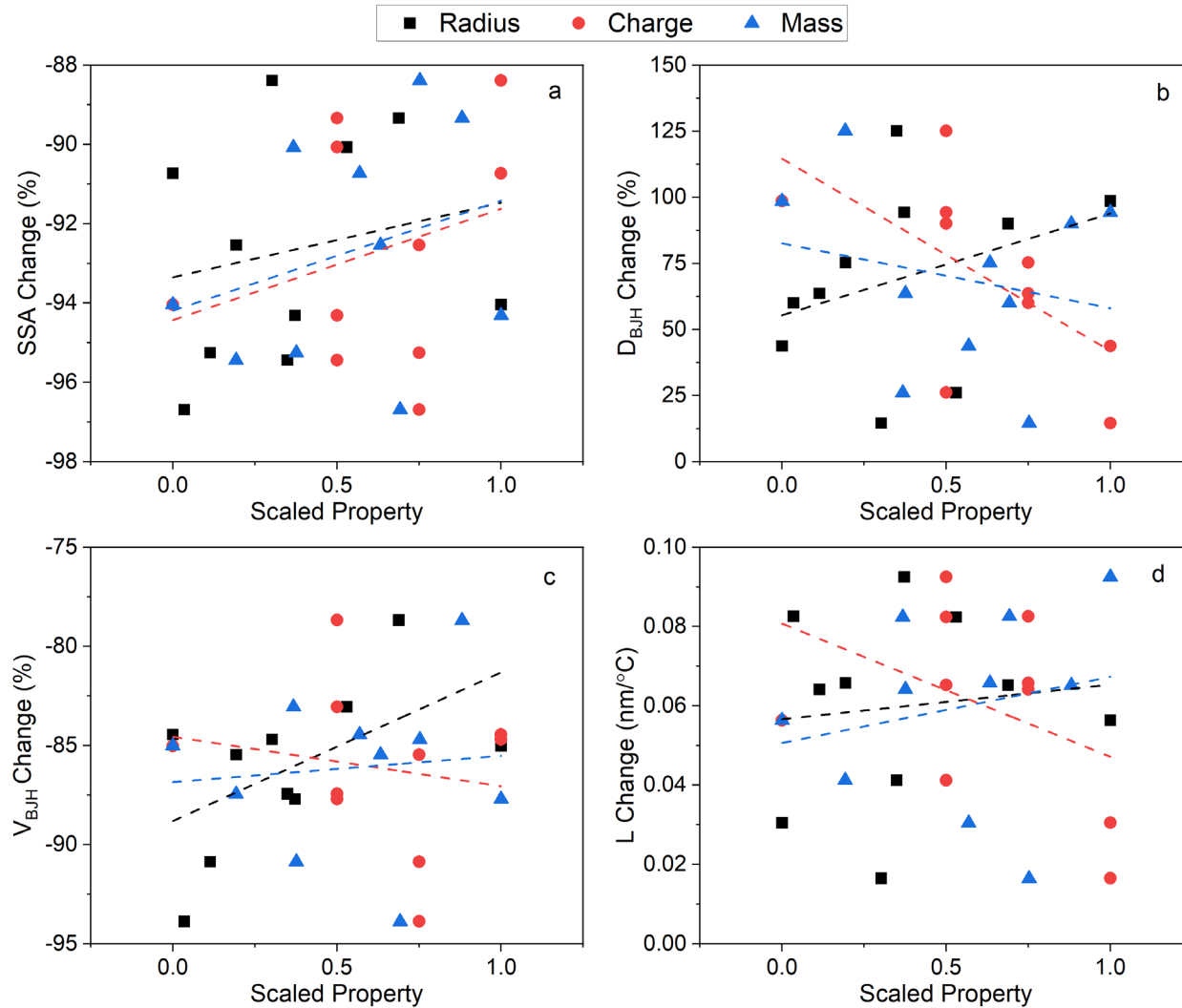


# Cation properties are not clearly related to absolute or relative stability



Property	Response		p-value
Radius			0.54
Charge	SSA	1000	0.50
Mass			0.44
Radius			0.04
Charge	V	1000	0.47
Mass			0.8
Radius			3.0E-04
Charge	D	1000	5.9E-04
Mass			0.41
Radius			0.83
Charge	L	1000	0.31
Mass			0.54

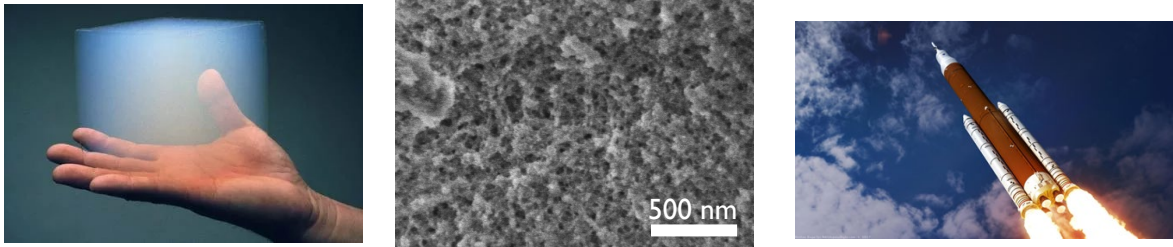
# Cation properties are not clearly related to absolute or relative stability



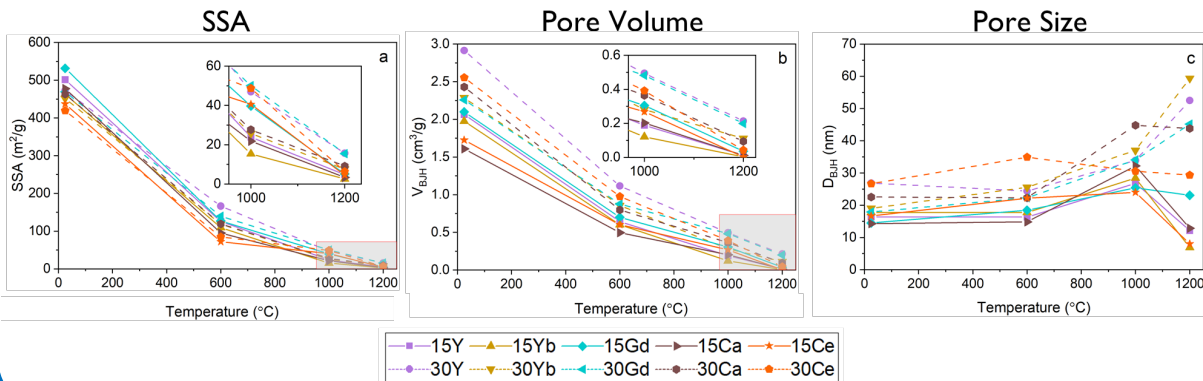
Property	Response	p-value
Radius	AD	0.57
Charge	% SSA	0.42
Mass	to 1000	0.40
Radius	AD	0.09
Charge	% V	0.63
Mass	to 1000	0.79
Radius	AD	0.32
Charge	% D	0.06
Mass	to 1000	0.54
Radius	600	0.76
Charge	Slope L	0.24
Mass	to 1200	0.55

# Summary

1. Aerogels are promising candidates for light weight, highly insulating materials in next-gen aerospace applications, but pore structure must be preserved to temperatures  $\geq 1200\text{ }^{\circ}\text{C}$

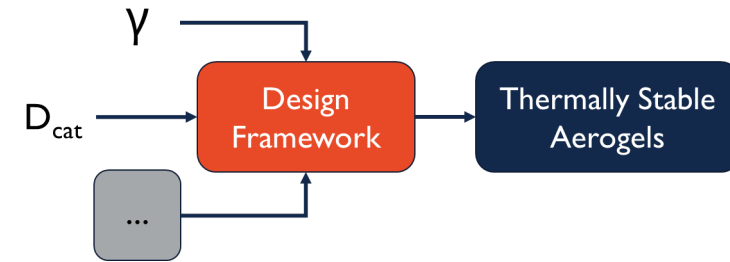


2. Increased dopant concentration from 15 to 30 mol% M/(M+Zr) reduces densification of the pore structure, with Gd and Y performing best.



# Looking Forward

1. Wider availability of material property data (surface energy, cation diffusivity, etc.) may help understand source(s) of variability in aerogel thermal stability.



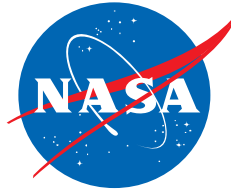
2. Considering the magnitude of improvements achieved by tuning composition, other routes beyond doping may be necessary to achieve thermal stability to temperatures  $\geq 1200\text{ }^{\circ}\text{C}$
3. Evaluation of new synthetic routes to aerogels with dramatically different chemistries and structures that offer improved thermal stability.

# Thank you for your attention! Special thanks to...

- Advisor: Dr. Jessica Krogstad (UIUC)
- Technical Collaborator: Dr. Jamesa Stokes (NASA GRC)
- Dr. Frances Hurwitz (NASA GRC, retired)
- Jordan Meyer (UIUC MatSE U-Grad)
- Krogstad Group members
- At NASA GRC: Dr. Haiquan (Heidi) Guo, Dr. Richard Rogers  
Jessica Cashman

## Funding:

- NASA Space Technology Research Fellowship  
(80NSSC18K1189)



## Facilities:

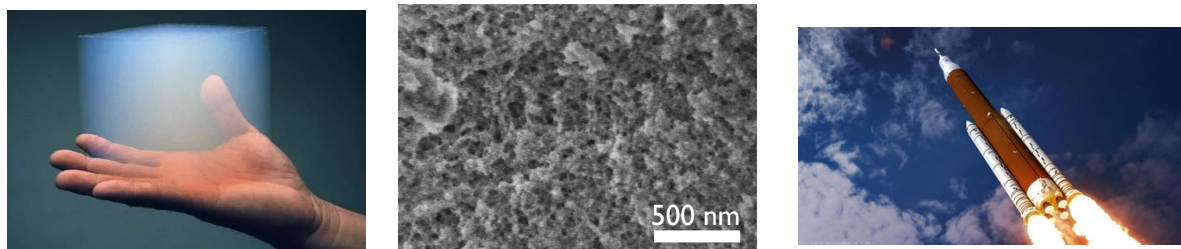
- Materials Research Laboratory, UIUC
- SCS Microanalysis Laboratory, UIUC
- NASA Glenn Research Center



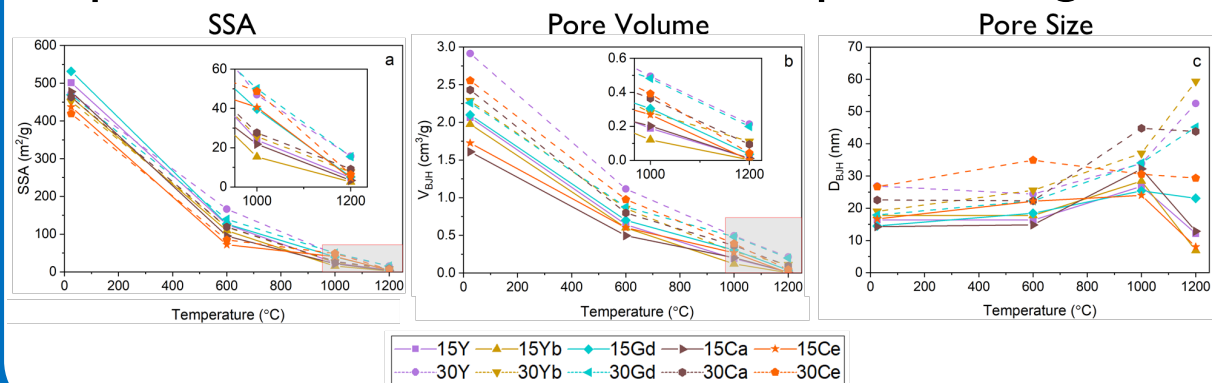


# Summary

1. Aerogels are promising candidates for light weight, highly insulating materials in next-gen aerospace applications, but pore structure must be preserved to temperatures  $\geq 1200\text{ }^{\circ}\text{C}$

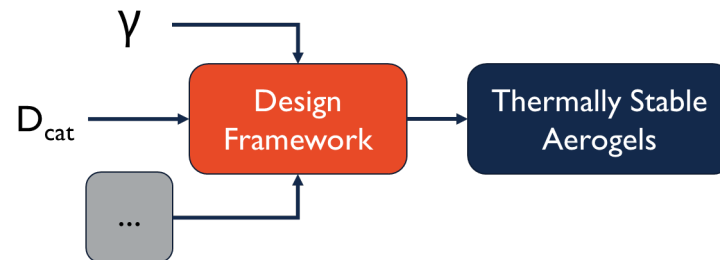


2. Increased dopant concentration from 15 to 30 mol% M/(M+Zr) reduces densification of the pore structure, with Gd and Y performing best.



# Looking Forward

1. Wider availability of material property data (surface energy, cation diffusivity, etc.) may help understand source(s) of variability in aerogel thermal stability.



2. Considering the magnitude of improvements achieved by tuning composition, other routes beyond doping may be necessary to achieve thermal stability to temperatures  $\geq 1200\text{ }^{\circ}\text{C}$
3. Evaluation of new synthetic routes to aerogels with dramatically different chemistries and structures that offer improved thermal stability.